RAPID COMMUNICATIONS

PHYSICAL REVIEW B VOLUME 45, NUMBER 3 15 JANUARY 1992-I

Defect generation and morphology of (001) Si surfaces during low-energy Ar-ion bombardment

M. V. Ramana Murty and Harry A. Atwater

Thomas J. Watson Laboratory of Applied Physics, California Institute of Technology, Pasadena, California 91125

(Received 15 October 1991; revised manuscript received 25 November 1991)

Low-energy Ar^+-ion bombardment of atomically rough (001) Si surfaces has been investigated using atomistic simulations. The simulations suggest that ions with energy less than 20 eV selectively displace surface atoms without causing bulk damage and further that the displacement yield is surface site specific in this energy range. Interpreted in the context of recent experimental kinetic data for Si-surface self-diffusion, the simulations imply that above room temperature the most important effect of ion bombardment on surface self-diffusion and surface morphology is an increase in the formation rate of single adatoms rather than enhancement of the migration component of surface self-diffusion.

Molecular-beam epitaxy offers an opportunity to grow structures with abrupt doping or composition profiles and strained layers. However, high growth temperatures may result in undesirable effects, such as dopant redistribution and strained-layer relaxation. Processes which employ bombardment of the growth surface with low-energy ions, such as direct-ion-beam deposition and ion-beam-assisted molecular-beam epitaxy have potential for growing epitaxial films at temperatures lower than is possible with conventional molecular-beam epitaxy. However, the potential of these techniques has not been fully exploited for lack of detailed information about how surface kinetic processes can be enhanced by ion bombardment without production of damage in the as-grown crystal. In this paper, we combine atomistic simulations with recent experimental surface kinetic data to (i) suggest possible mechanisms for enhancement in surface self-diffusion, (ii) rule out others, (iii) predict the ion energy regime in which surface-diffusion enhancement is possible without bulk damage, and (iv) suggest that the surface-displacement yield is site specific.

Changes in surface morphology[1] and kinetics of strain modification[2] in epitaxial growth of Ge and Ge_xSi_{1-x} have been attributed to ion-beam generated defects. Several different phenomena may occur as a result of low-energy ion bombardment during growth, including enhanced adatom diffusion, sputtering, dissociation of small islands and generation of alternate nucleation sites. Although there is great interest in modification of surface kinetics, in order to grow device-quality films, it is necessary to limit the bulk damage caused by the impinging ion beam.

Low-energy collisions in a solid typically involve many atoms and simulation by Monte Carlo or binary collision[3] methods may not be sufficiently accurate. Molecular-dynamics (MD) simulations, where every atom interacts with all other atoms (within a certain cutoff radius), can be used to delineate the essential kinetic processes in the prompt regime during ion-assisted epitaxy. Previous MD studies of silicon include initial stages of epitaxy,[4] sputtering by keV-range Ar^+ ions,[5] direct-ion-beam deposition using 10-eV Si ions[6] and observation of surface channeling on (111) Si.[7] These studies have employed idealized atomically smooth surfaces. Real surfaces are often not atomically smooth and include various structures such as vacancies, single adatoms, dimer strings, ledges, and kink sites. It is reasonable to suppose that at ion energies near the displacement threshold that some or all of the effects of ion bombardment may occur preferentially at these structures. A better understanding of the principal effects of ion bombardment can be gained by studying the interactions of the incident beam with a surface consisting of the above-mentioned structures. MD calculations are generally limited at present to small ensembles (typically 10^3) and short time durations (typically a few picoseconds) which does not permit the study of diffusive processes. We also note that because of the well-known possible shortcomings of classical adiabatic potentials,[8] the results of MD simulations must in most instances be interpreted cautiously, and qualitatively rather than quantitatively. However, the qualitative effects of cascade dynamics on surface and bulk defect structures can be estimated and can be coupled to later diffusive processes with experimentally determined surface kinetic data.

A central feature of cascade dynamics is the numerous overcoordinated and undercoordinated configurations in which the atoms are found. The chosen interatomic potential must be able to describe not only the atomic interactions near the equilibrium position, but also the low- and high-density regions occurring in the collision cascade. The semiempirical Tersoff potential[9] has been used to model Si because it gives a good fit to the crystalline structures of Si with coordination numbers higher and lower than the diamond cubic lattice. The potential also gives reasonable agreement with the experimental dimer length of the (2×1) reconstruction on the (001) Si surface, and for bulk vacancy and interstitial energies. In our work, a sharp cutoff at 0.32 nm ($f_{ij}=1$, $r_{ij}<0.32$ nm, and $f_{ij}=0$, $r_{ij}>0.32$ nm in Tersoff potential[9]) was used for the Si-Si interaction. The Ar-Si interaction was taken to be purely repulsive, $V_{\text{Ar-Si}}=A\exp(-\lambda r_{\text{Ar-Si}})$ with $A=1830.8$ eV, $\lambda=20$ nm^{-1} and was cutoff at 0.4 nm.

Ion-beam-induced defect production was estimated from the smooth (2×1) reconstructed (001) Si, a dimer pair and the edge and the center of a dimer string placed on (001) Si. The choice of these structures was guided by scanning-tunneling-microscope (STM) images[10] of reconstructed (001) Si surfaces. There are, in principle, several

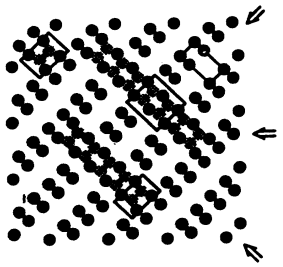

FIG. 1. The three defect structures placed on the (001) Si surface. The rectangles drawn around each structure indicate the area in which the ions were incident. All ions were incident at 45° to the plane of the crystal and the arrows indicate the azimuths.

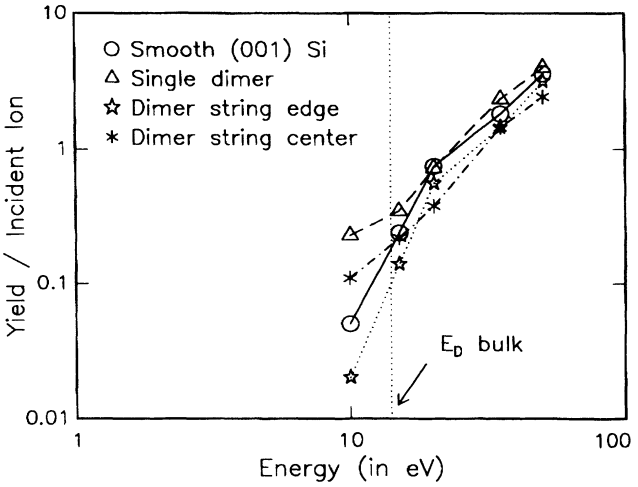

FIG. 2. The total displacement yield vs energy for the defect structures. The lines are spline fits to guide the eye.

choices for the position of these defect structures on (001) Si surface. The positions shown in Fig. 1 corresponded to configurations with minimum energy calculated using the Tersoff potential and these were used for studying the effects of ion bombardment.

In the simulations, ions were incident at 45° with respect to the plane of the surface along three different azimuths—parallel to the dimer rows, perpendicular to the dimer rows and one at an azimuthal angle 45° from these directions as indicated in Fig. 1. Five different ion energies—10, 15, 20, 35, and 50 eV were employed. A total of 102 simulations were carried out for each energy with each structure. The incident ion impact points were chosen at random within the rectangle drawn around each structure in Fig. 1. For the smooth (001) Si surface, the impact parameter range is the (2×1) unit cell. The average and the standard deviation of the impact parameter along with the size of the simulation crystallite for each of these structures is listed in Table I. We see that these are sufficiently close to make a fair comparison since a collision described with a single impact parameter does not provide a general description of defect yields. The initial substrate temperature was 0 K and simulations were carried out for a period of 1.0 ps.

In the simulation results described below, the layer containing the atoms placed on the (2×1) surface is referred to as layer 0, the (2×1) surface is referred to as layer 1, the one below it as layer 2, and so on up to layer 24.

Production of atomic displacements, interstitials, and sputtered atoms are typical events observed in a collision cascade. Our criterion for a displacement is met if there is no Si atom within the hard-sphere radius, i.e., a sphere of radius equal to half the equilibrium Si-Si bond length, within the original lattice site. Figure 2 shows the total displacement yield observed at different ion energies for the different structures. The results here are all averaged over 102 simulations. With 10-eV ions, the yields from the different structures are spread over a wide range. At higher energies, surface displacements constitute only a small fraction of the total displacements and the surface defect structure is expected to have a smaller effect on the collision cascade. This results in a steady decline in the difference in yield between the different structures with increase in energy. The bulk displacement energy E_D for Si is often considered to be approximately $E_D = 14$ eV. The large spread in calculated displacement yields for different structures at 10 eV compared to energies greater than E_D is consistent with this estimate.

Figure 3(a)–3(d) shows the depth distribution of displacements in the crystal. With 10-eV ions, the displacements are almost exclusively confined to the defect layer (layer 0). For ions incident on smooth (001) Si, displacement yields greater than 0.05 are observed up to the third, fourth, and fifth layers with 20-, 35-, and 50-eV ions, respectively. It should be noted that the number of displacements in layer 0 can be at most two for the dimer pair. No sputtering was observed from any of the structures in the energy range considered.

The surface displacement threshold energy is presumed to be a fraction of the bulk displacement energy and highly dependent on surface structure. The MD calculations suggest that at 10 eV, the displacements in the dimer pair

TABLE I. Impact parameters used with different surface defect structures.

Surface structure	Crystallite size (in unit cells)	Impact parameter Average (nm)	Standard deviation (nm)	Measured with respect to atoms in the
Smooth (001) Si	6×6×6	0.116	0.056	(2×1) cell
Dimer pair	6×6×6	0.130	0.064	placed dimer
Dimer string edge	8×8×6	0.112	0.052	placed dimers
Dimer string center	8×8×6	0.115	0.059	placed dimers

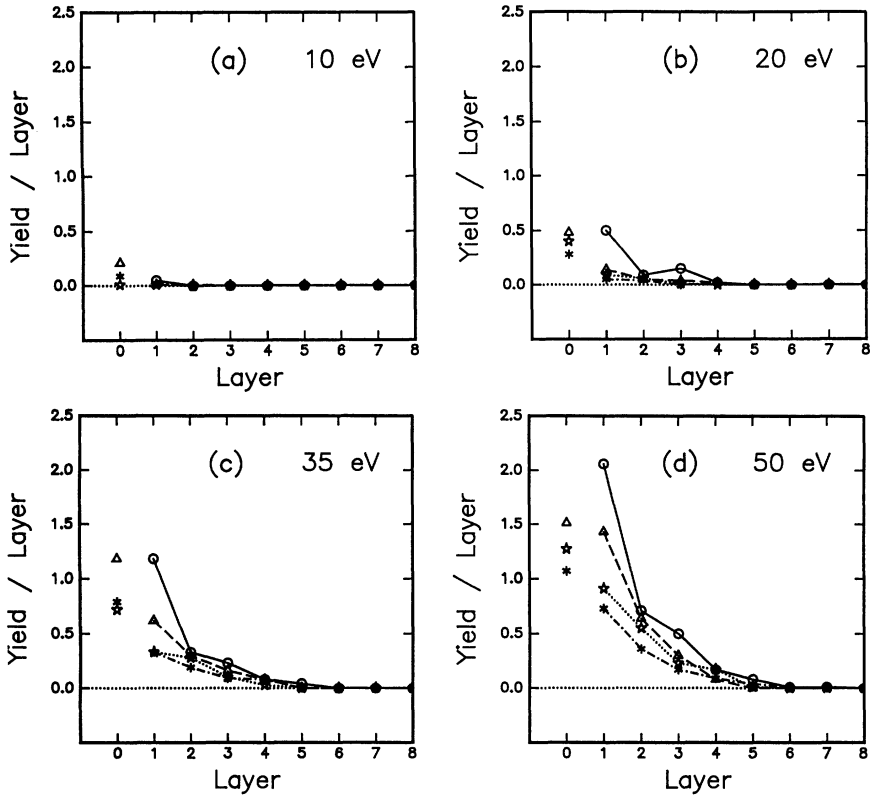

FIG. 3. The distribution of displacements in the substrate at (a) 10 eV, (b) 20 eV, (c) 35 eV, and (d) 50 eV. The four symbols refer to smooth (001) Si (○), dimer pair (△), dimer string edge (☆), and dimer string center (∗). Displacements in layer 0 are those from the defect placed on the surface.

are due largely to surface displacements. It should be noted that these displacement yields were observed at the end of the simulation period of 1 ps and that the substrate temperature will determine the annealing dynamics and, hence, any observable defect generation on a laboratory timescale.[11] The calculated difference in yields from different defect structures at low energies indicate that surface displacement yields are site specific and any experimental determination of threshold energies must account for this fact.

Figure 4(a) shows the ratio R of displacements in layer 0 to all other layers from the defect structures. The ratio changes from about 2–3 for 20-eV ions to 0.6–0.8 for 50-eV ions for the different structures. In Fig. 4(b), the number of broken dimers (only from the placed dimers) is shown for the different energies. It is seen that 35- and 50-eV ions give a high dimer breaking efficiency but also cause significant bulk damage. The lower value of R from the center of the dimer string at 15 eV compared to 20 eV is presumably due to an insufficient number of simulations. The absolute number of displacements with 10- and 15-eV ions was too low to give a value of R without a large error. These results suggest that ions with energy less than 20 eV selectively displace surface atoms. A large surface-to-bulk displacement ratio is highly desirable because it may allow modification of surface kinetics without causing bulk damage. Previous results[12] suggest that the surface-to-bulk displacement ratio is greater with ions incident at 45° to the plane of the crystal compared to normal incidence. If we assume that surface vacancies up to second layer can be filled by migrating adatoms and interstitials, then it is reasonable to assume that ions with energy less than 20 eV can alter surface kinetics without causing bulk damage. Recently, successful epitaxy has been reported at temperatures around 300 °C in low-energy bias sputtering experiments.[13,14] The best quality films were obtained with ion energies less than 30 eV.

Recent experimental[15] and theoretical[16] studies indicate that two atoms, in a dimer pair, form a stable cluster

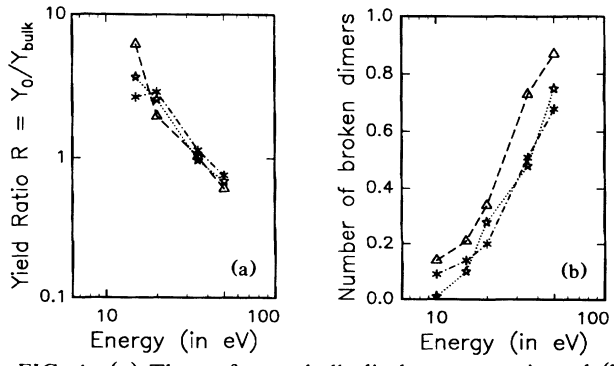

FIG. 4. (a) The surface-to-bulk displacement ratio and (b) the average number of broken dimers per incident ion (only from the placed dimers) for the different defect structures.

on (001) Si. Single adatoms, on the other hand, are highly mobile at $T \geq 300$ K. Adatom diffusion is also highly anisotropic, the fast direction being along the dimer rows. The activation energy and prefactor for single adatom diffusion have been estimated[15] to be about 0.67 eV and 10^{-3} cm^2/s respectively. After deposition, adatoms migrate to ledges, adsorb at existing clusters or nucleate two-dimensional islands. These different processes determine the lifetime of an adatom (before it forms or joins a stable cluster). At typical ion fluxes employed in experiments ($\sim 10^{16}/cm^2 s$), the interarrival time of ions is very large compared to the lifetime of an adatom at $T \geq 300$ K. During ion bombardment, the probability of striking an adatom becomes significant only at $T \leq 300$ K.

These results suggest the following phenomenological view of surface modification by low energy ion bombardment during growth. Silicon homoepitaxy occurs in a layer-by-layer or Frank–van der Merwe mode, a fact confirmed by observation of reflection high-energy electron-diffraction oscillations[17] and scanning tunneling microscopy.[10] During growth, single atoms are adsorbed onto terraces, and in the absence of island nucleation, the adatom diffusivity is determined only by its migration rate. By contrast, the activation energy for diffusion of an atom in a ledge site, kink site, or even a single dimer consists of two parts: (a) formation energy, which is necessary to desorb an atom from an existing island, and (b) migration energy. In the simulations, observations of Si atom recoils show that, on average, they move only a lattice site or two from their original position after an ion impact. Comparison of the recoil atom trajectories and STM-derived kinetic data on adatom diffusion[10] clearly show that the thermal motion of single adatoms dominates any ion induced migration at $T \geq 300$ K. This suggests that ion bombardment does not enhance the migration component of diffusion except for ion incidence along special, surface channeling directions.[7] However, the most important effect of low-energy ion bombardment is the beam-induced creation of single adatoms which corresponds to the provision of the adatom formation energy (ledge-terrace desorption energy or dimer-breaking energy) by the incident ion.

In conclusion, the interaction of low-energy Ar^+ ions with several defect structures on (001) Si has been investigated using molecular-dynamics simulations. The displacement yields for different defect structures have been found to be different. Ions with energy less than 20 eV were found to selectively displace surface atoms with a displacement yield that is site specific and without causing bulk damage. Combined with recent kinetic data[10] about surface self-diffusion, the simulations suggest that the migration component of single adatom diffusion is not significantly enhanced by ion bombardment at typical epitaxial temperatures (600–800 K). The most important effect of ion bombardment on surface morphology is the increased formation rate of single adatoms. This may lead to smoother surfaces by suppression of island nucleation or enhanced coarsening above room temperature, where adatom diffusivities are large.

We thank M. G. Lagally for supplying data prior to publication and helpful discussions. This work was supported by National Science Foundation Grant No. DMR-8958070 and the AT&T Foundation. M.V.R.M. also acknowledges support through the Powell Foundation.

[1] J. Y. Tsao, E. Chason, K. M. Horn, D. K. Brice, and S. T. Picraux, Nucl. Instrum., Phys. Res. Sect. B **39**, 72 (1989).

[2] C. J. Tsai, H. A. Atwater, and T. Vreeland, Appl. Phys. Lett. **57**, 2305 (1990).

[3] D. K. Brice, J. Y. Tsao, and S. T. Picraux, Nucl. Instrum., Phys. Res. Sect. B **44**, 68 (1989).

[4] D. W. Brenner and B. J. Garrison, Surf. Sci. **198**, 151 (1988).

[5] R. Smith, D. E. Harrison, and B. J. Garrison, Phys. Rev. B **40**, 40 (1989).

[6] M. Kitabatake, P. Fons, and J. E. Greene, J. Vac. Sci. Technol. A **8**, 3726 (1990).

[7] B. W. Dodson, J. Vac. Sci. Technol. B **5**, 1393 (1987).

[8] B. W. Dodson, Crit. Rev. Solid State Mater. Sci. **16**, 115 (1990).

[9] J. Tersoff, Phys. Rev. B **38**, 9902 (1988).

[10] M. G. Lagally, *Kinetics of Ordering and Growth at Surfaces* (Plenum, New York, 1990).

[11] S. T. Picraux, D. K. Brice, K. M. Horn, J. Y. Tsao, and E. Chason, Nucl. Instrum., Phys. Res. Sect. B **48**, 414 (1990).

[12] M. V. R. Murty, H. S. Lee, and H. A. Atwater, Mater. Res. Soc. Symp. Proc. **193**, 301 (1990).

[13] G. K. Wehner, R. M. Warner, Jr., P. D. Wang, and Y. H. Kim, J. Appl. Phys. **64**, 6754 (1988).

[14] T. Ohmi, T. Ichikawa, H. Iwabuchi, and T. Shibata, J. Appl. Phys. **66**, 4756 (1989).

[15] Y. M. Mo, J. Kleiner, M. B. Webb, and M. G. Lagally, Phys. Rev. Lett. **66**, 1998 (1991).

[16] G. Brocks, P. J. Kelly, and R. Car, Phys. Rev. Lett. **66**, 1729 (1991).

[17] T. Sakamoto, N. J. Kawai, T. Nakagawa, K. Ohta, and T. Kojima, Appl. Phys. Lett. **47**, 617 (1985).